Research Article | Vol. 27, No. 21 / 14 October 2019 / Optics Express 29738
Optics EXPRESS

Superluminal Raman laser with enhanced cavity length sensitivity

ZIFAN ZHOU,[1,*] MINCHUAN ZHOU,[2] AND SELIM M. SHAHRIAR[1,2]

[1]Department of EECS, Northwestern University, Evanston, IL 60208, USA
[2]Department of Physics and Astronomy, Northwestern University, Evanston, IL 60208, USA
[*]zifanzhou2012@u.northwestern.edu

Abstract: We demonstrate experimentally a superluminal ring laser based on optically pumped Raman gain, and a self-pumped Raman depletion for producing anomalous dispersion, employing two isotopes of rubidium. By fitting the experiment data with the theoretical model, we infer that the spectral sensitivity of the superluminal Raman laser to cavity length change is enhanced by a factor of more than a thousand, compared to a conventional laser.

1. Introduction

In recent years, we have been investigating the use of critically tuned anomalous dispersion for a range of metrological applications [1–14]. Of particular interest in this context is the superluminal laser [1–8], for which the laser frequency shift due to cavity length perturbation can be enhanced by several orders of magnitude. The group velocity in a superluminal laser is larger than the speed of light in vacuum, without violating causality or special relativity [15]. Making a superluminal laser requires the use of a gain medium which is tailored in a way so that the laser experiences steep negative dispersion. Recently, we demonstrated experimentally [8] a superluminal laser using a Diode-Pumped Alkali Laser (DPAL) gain medium, coupled with a with a Raman resonance induced depletion. In this DPAL based superluminal laser, the spectral sensitivity to change in the cavity length was found to be enhanced by a factor of ~190. While achieving a much larger factor of enhancement in sensitivity should be possible in the DPAL based superluminal laser, it is not well suited for some applications, such as rotation sensing [2], that requires the operation of two spatially overlapping but counter-propagating lasers to operate in the same cavity without any cross talk. This is due to the fact that the gain in a DPAL medium is bi-directional. Here, we demonstrate a new type of superluminal laser for which the gain is unidirectional, thus making it suitable for such applications. Specifically, in this scheme, the main gain mechanism is a Raman population inversion between two hyperfine ground states in ^{85}Rb, produced via optical pumping. Application of a Raman gain pump then produces Raman gain for a probe, which is maximized when it is two-photon resonant with the Raman pump. The width of the Raman gain profile is relatively narrow (few MHz), and can be tailored by adjusting the operational parameters. We use this gain to realize first a Raman laser [16,17]. The requisite dip in the gain spectrum [1] is then produced by applying another laser, called the Raman depletion pump. The frequency of this Raman depletion pump is chosen to be such that the Raman laser is two-photon resonant with this pump with respect to the two hyperfine ground states in ^{87}Rb. For suitable choice of parameters, the Raman laser experiences a narrow band absorption from ^{87}Rb, thus producing a dip in the gain profile. This is called self-pumped Raman depletion. Since co-propagating (counter-propagating) Raman resonance is highly insensitive (sensitive) to the Doppler broadening in atomic vapor, both Raman gain and Raman depletion only efficiently work when the Raman laser is co-propagating with the Raman gain pump and the Raman depletion pump, thus making the process unidirectional. If two separate gain cells are used in the same cavity, each with its own Raman gain and depletion pumps, then two counter-propagating superluminal ring lasers can be realized without any cross

#373269 https://doi.org/10.1364/OE.27.029738
Journal © 2019 Received 19 Jul 2019; revised 19 Sep 2019; accepted 19 Sep 2019; published 1 Oct 2019

Optics EXPRESS

talk, by making use of polarizing beam splitters to insert and remove the pumps for one cell before they can enter the other cell. This is made possible by the fact that the polarization of the resulting Raman laser is orthogonal to that of the Raman gain pump and the Raman depletion pump (which are polarized in the same direction).

2. Experimental configuration

The relevant laser fields and the energy levels in both isotopes of Rb are shown in Fig. 1(a). In ^{85}Rb, we denote the relevant energy levels as follows:$|1\rangle \equiv \{5S_{1/2}, F = 2\}$, $|2\rangle \equiv \{5S_{1/2}, F = 3\}$, $|3\rangle \equiv 5P_{1/2}$, and $|4\rangle \equiv 5P_{3/2}$. The optical pump is tuned to the $|1\rangle \leftrightarrow |4\rangle$ transition, and kept stable using a peak-lock servo. This creates a condition where the population of level $|2\rangle$ is greater than that of level $|1\rangle$. The Raman gain pump A is tuned above the $|2\rangle \leftrightarrow |3\rangle$ transition, by $|\Delta_1| \simeq 1GHz$. Under this condition, a relatively broad gain is produced for a probe applied along the $|1\rangle \leftrightarrow |3\rangle$ transition. The peak of this gain occurs when the difference in frequency between the Raman gain pump A and the probe matches the frequency difference between $|1\rangle$ and $|2\rangle$. In the presence of a cavity tuned to this frequency, this system will produce a Raman laser at this probe frequency.

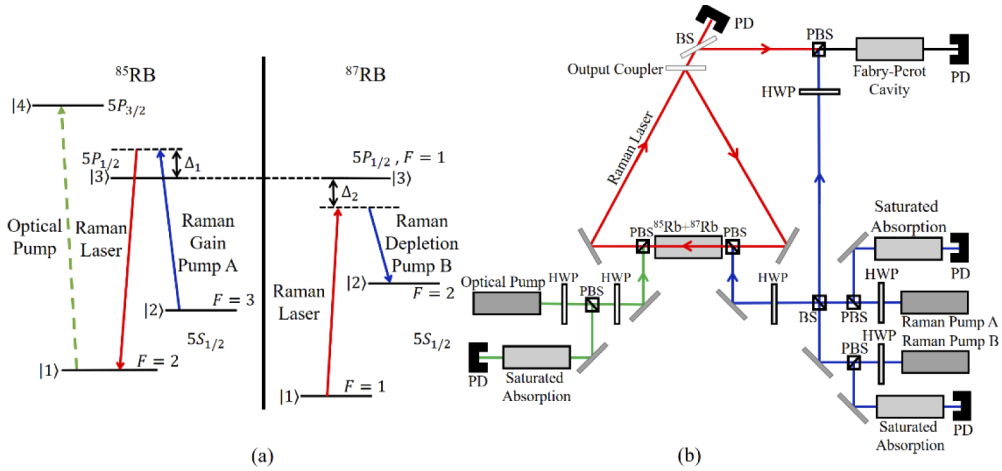

Fig. 1. (a) Energy levels and optical fields in the gain medium and (b) the schematic of the experiment configuration.

In ^{87}Rb, we denote the relevant energy levels as follows: $|1\rangle \equiv \{5S_{1/2}, F = 1\}$, $|2\rangle \equiv \{5S_{1/2}, F = 2\}$, $|3\rangle \equiv \{5P_{1/2}, F = 1\}$. Here, we make use of the self-pump Raman depletion process, which works as follows. The Raman depletion pump B is tuned below the $|2\rangle \leftrightarrow |3\rangle$ transition by an amount $|\Delta_2|$. This creates a condition where the population of level $|1\rangle$ is greater than that of level $|2\rangle$. Consider now the application of a probe along the $|1\rangle \leftrightarrow |3\rangle$ transition. When the difference in frequency between the Raman depletion pump B and this probe matches the frequency difference between $|1\rangle$ and $|2\rangle$, the probe will experience maximum Raman depletion. Thus, the Raman laser produced in ^{85}Rb will experience this peak Raman depletion if the value of $|\Delta_2|$ is chosen to be ~1.280 GHz, given that $|\Delta_1| \simeq 1GHz$. Under this condition, the frequency difference between the Raman gain pump A and the Raman depletion pump B, denoted as Δ_{AB}, will match the difference between the ground state hyperfine splittings of ^{87}Rb and ^{85}Rb, which are 6.834682 GHz and 3.035732 GHz, respectively. When rounded to three decimal points, the value of Δ_{AB} is 3.799 GHz under this condition. If $|\Delta_1|$ is increased by an amount $|\delta|$, then $|\Delta_2|$ also has to be reduced by $|\delta|$ so that Δ_{AB} remains unchanged. Note that the sign of Δ_1 is positive and the sign of Δ_2 is negative.

Optics EXPRESS

The schematic of the experiment apparatus is shown in Fig. 1(b). We make use of a cell filled with natural Rubidium vapor, which contains 72% ^{85}Rb and 28% ^{87}Rb and is heated up to 150 °C, as the gain medium of a triangular ring laser with a cavity length of 61 cm. The cavity is composed of two plane perfect reflectors and a plane output coupler with a reflectivity of 54.5%. The estimated empty cavity linewidth is ~70 MHz. A lens, with a focal length of 75 cm, is inserted into the cavity to produce a stable cavity mode. The three pump lasers are coupled into the cavity through polarizing beam splitters (PBS). The power in each Raman pump is 5 mW, and the power in the optical pump is 315 mW. All three pump beams are focused (not shown) to match the cavity mode. The output of the laser is split into two parts. A small fraction (~5%) of the output is received by a photo detector (PD) used to measure the output power, and the rest of the output is combined with the two Raman pumps and sent into a Fabry-Perot cavity to characterize its properties. There are three saturated absorption set ups for the three pump lasers to keep track of their frequencies.

3. Theoretical modeling

To quantify the sensitivity enhancement of a superluminal laser, we developed a theoretical model to simulate its behavior. The simulation is based on the N-level algorithm [18,19] developed previously by us, and considers all the hyperfine levels in both $5S_{1/2}$ and $5P_{1/2}$ manifolds, as shown in Fig. 2(a). For simplification, the optical pumping in ^{85}Rb is modeled as an effective decay rate, denoted as $\Gamma_{\rm op}$, between the two hyperfine states in the $5S_{1/2}$ manifold, and its value is calculated as follows. We first consider a 3-level system shown in Fig. 2(b). Here, we denote the relevant energy levels as follows: $|1\rangle \equiv \{5S_{1/2}, F = 1\}$, $|2\rangle \equiv \{5S_{1/2}, F = 2\}$, and $|3\rangle \equiv 5P_{3/2}$. The optical pump is tuned to the resonance of the $|1\rangle \leftrightarrow |3\rangle$ transition. The optical pumping beam is linearly polarized, which is equivalent to a superposition of left and right circular polarizations. We define the saturation intensity as $I_{sat} = \alpha I_{sat,max}$, where $I_{sat,max} \simeq 1.67 mW/cm^2$ is the saturation intensity for the cycling transition that couples $5S_{1/2}, F = 3, m_F = 3$ to $5P_{3/2}, F = 4, m_F = 4$ levels. The value of α is determined by carrying out an average of the squares of the matrix element between the Zeeman sublevels within the $5S_{1/2}, F = 2$ hyperfine state and the F'=1, 2 and 3 hyperfine states within the $5P_{3/2}$ manifold. Since the optical pumping beam is tuned to the center of the Doppler broadened transition between the $5S_{1/2}, F = 2$ level and the $5P_{3/2}$ manifold, we treat the later as a single energy level. We assume, for simplicity, that the rate of decay from $5P_{3/2}$ to $5S_{1/2}, F = 2$ and $5S_{1/2}, F = 3$ are equal, indicated as $\Gamma/2$ in Fig. 2(b), where $\Gamma/2\pi \simeq 6 MHz$. We also assume a collisional decay from $|1\rangle$ to $|2\rangle$ and $|2\rangle$ to $|1\rangle$, at the rate of γ_{12} and γ_{21}, respectively. Since the steady state population of states $|1\rangle$ and $|2\rangle$ are nearly equal at the operation temperature, we assume $\gamma_{12} \simeq \gamma_{21} \equiv \gamma$. Based on the linewidth of a typical Raman transition in such a system [11], we assume the value of $\gamma/2\pi$ to be ~1 MHz. Under these assumptions, we solve the Liouville equation in steady state, to determine the populations of $|1\rangle$ and $|2\rangle$, denoted as ρ_1 and ρ_2, respectively. If we summarize the role of the optical pumping beam as producing a net decay at the rate of $\Gamma_{\rm op}$ from $|1\rangle$ to $|2\rangle$, then we can write that $(\gamma_{12} + \Gamma_{op})/\gamma_{21} = \rho_2/\rho_1$. For $\gamma_{12} \simeq \gamma_{21} \equiv \gamma$, we thus get $\Gamma_{op} = \gamma(\rho_2 - \rho_1)/\rho_1$.

For the Raman gain process in ^{85}Rb, we model the D_1 manifold as a 4-level system, as illustrated in the left panel of Fig. 2(a). We denote the relevant energy levels as follows: $|1\rangle \equiv \{5S_{1/2}, F = 2\}$, $|2\rangle \equiv \{5S_{1/2}, F = 3\}$, $|3\rangle \equiv \{5P_{1/2}, F = 2\}$, and $|4\rangle \equiv \{5P_{1/2}, F = 3\}$. We again assume the natural decay from $|3\rangle$ and $|4\rangle$ to $|1\rangle$ and $|2\rangle$ to be at the same rate of $\Gamma/2$. The collisional decay rates between $|1\rangle$ and $|2\rangle$ are again assumed to be $\gamma_{12} \simeq \gamma_{21} \equiv \gamma = 2\pi \times 10^6 \text{sec}^{-1}$. The Raman gain pump A is linearly polarized and excites both $|2\rangle \leftrightarrow |3\rangle$ and $|2\rangle \leftrightarrow |4\rangle$ transitions, and is tuned above the $|2\rangle \leftrightarrow |3\rangle$ transition, by $|\Delta_1| \simeq 1 GHz$. The saturation intensity for each transition is calculated individually using the averaging approach discussed above. The Raman laser field is nominally tuned to be two-photon resonant with the Raman gain pump A and excites both $|1\rangle \leftrightarrow |3\rangle$ and $|1\rangle \leftrightarrow |4\rangle$ transitions. However, during the calculation, we set the frequency and

Optics EXPRESS

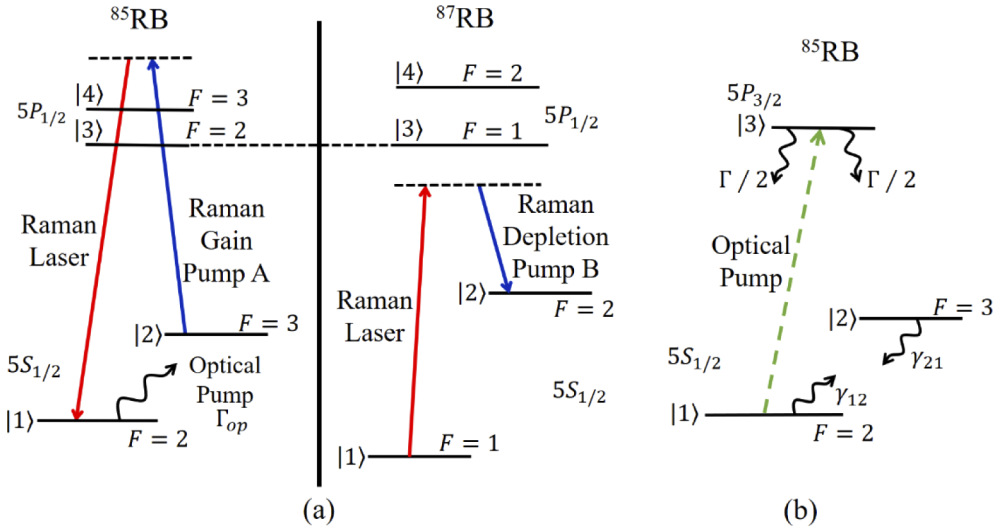

Fig. 2. (a) Theoretical model of the superluminal Raman laser, and (b) the 3-level system for calculating the optical pumping rate between the hyperfine levels in the $5S_{1/2}$ manifold of ^{85}Rb.

the intensity of the Raman laser field to be variables that need to be determined using an iterative algorithm [8,19].

Similarly, for the Raman depletion process in ^{87}Rb, we model the D_1 manifold as another 4-level system. The relevant energy levels are denoted as follows: $|1\rangle \equiv \{5S_{1/2}, F = 1\}$, $|2\rangle \equiv \{5S_{1/2}, F = 2\}$, $|3\rangle \equiv \{5P_{1/2}, F = 1\}$, and $|4\rangle \equiv \{5P_{1/2}, F = 2\}$. The natural decay rates from $|3\rangle$ and $|4\rangle$ and the collisional decay rates between $|1\rangle$ and $|2\rangle$ are assumed to be the same as those in ^{85}Rb. The Raman depletion pump B is tuned below the $|2\rangle \leftrightarrow |3\rangle$ transition, by $|\Delta_2| \simeq 1.280GHz$. To match the experimentally measured output power of the Raman laser, we first assume that the frequency of the Raman depletion pump B and that of the Raman gain pump A are fixed. By solving the Liouville equation and the equations of motion for a single mode laser in a self-consistent manner [8,19], we can obtain the steady state solutions of the intensity and the frequency of the Raman laser field. To calculate the sensitivity of the Raman laser under this condition, we manually apply a small perturbation in the cavity length (dL). The simulation can find the output frequency shift (df) of the Raman laser. Here we define the sensitivity of the Raman laser as S_{RL}=df/dL. The sensitivity enhancement can be then expressed as $S_{\mathrm{RL}}/S_{\mathrm{EM}}$, where S_{EM} is the sensitivity of an empty cavity with the same length as that of the Raman laser. We then vary the frequency of the Raman depletion pump B around Δ_2 (with the frequencies of the Raman gain pump A and the optical pump fixed). The simulation can determine the output power of the Raman laser at each single frequency of the Raman pump B. By solving for all the frequencies within the experiment frequency scan, we can find the theoretical output power of the Raman laser as a function of the frequency difference between the two Raman pumps.

As noted earlier, for each isotope, the Raman pump is linearly polarized, which is a superposition of left- and right-circular polarizations. For the left-circular polarization, the allowed transitions correspond to all Zeeman sublevels that meet the condition of $m' - m = -1$, where m' (m) is the angular momentum quantum number for a sublevel in an upper (lower) hyperfine level. Similarly, for the right-circular polarization, the allowed transitions correspond to all Zeeman sublevels that meet the condition of $m' - m = 1$. We have taken into account the dipole matrix elements of all of these transitions to estimate the effective Rabi frequency for the Raman pump. Of course, this approach is an approximate one. A more rigorous approach would require a multi-level

Optics EXPRESS

calculation, taking into account all the Zeeman sublevels in all the hyperfine states. In other contexts, we have carried out such calculations, using an algorithm develop by our group [18]. However, such a computation is prohibitively time consuming for the case considered, since we are employing an iterative algorithm [19] to solve for the steady state laser power and laser frequency. Nonetheless, in the near future, we plan to carry out such a detailed model for the superluminal laser.

4. Results

Figure 3(a) shows the experiment data and the simulation result of the output power of the Raman laser, as functions of the frequency difference between the two Raman pumps. The dip is centered at ~3.799 GHz, as explained earlier. The noise present in the experimental data is due to the power fluctuation of the Raman laser, which could be caused by the temperature instability and the vibrations of the optical components. It should also be noted that the frequencies of the Raman pumps are not locked. There are several ways the frequencies of the Raman pumps can be stabilized. For example, one could lock a maser laser to an atomic transition, and then use the technique of offset phase locking to produce a stable frequency difference between each of the Raman pump lasers and the master laser. Such an approach will be used when attempting the use of this technique for precision metrology in the near future.

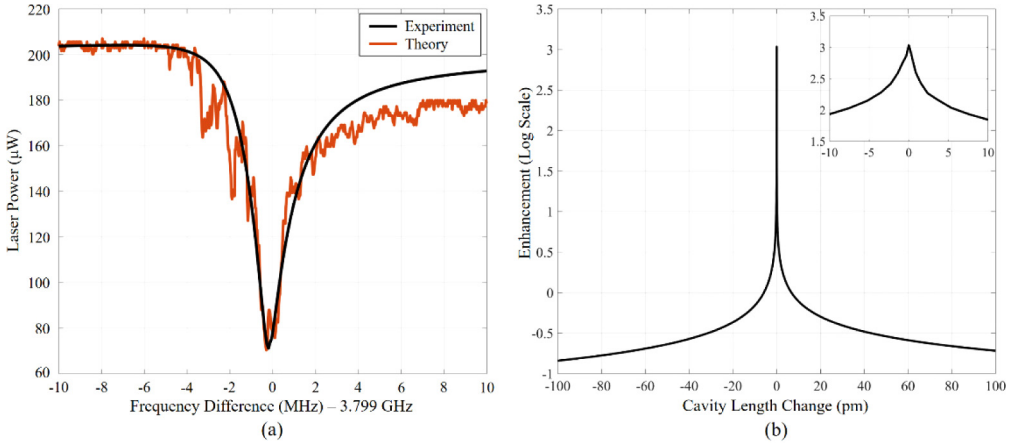

Fig. 3. (a) Experimental and theoretical results of the output power of the superluminal Raman laser as functions of the frequency difference between the two Raman pumps and (b) theoretical estimation of the enhancement of cavity length sensitivity at the two-photon resonance frequency in ^{87}Rb.

In the experiment, the value of Δ_1 is determined by using the following procedure. First, the frequency of the laser (i.e., the Raman gain pump) is scanned by varying the drive current linearly. The Raman lasing is observed at a particular point in this scan. A part of the Raman gain pump is passed through a saturated absorption cell, as shown in Fig. 1(b). The saturated absorption spectrum is observed during the whole scan. From the known separations between the observed resonances, the value of the change in the frequency for a given change in the current is determined. This number is then used to determine the value of Δ_1. The value of Δ_2 is determined by following a similar procedure. Specifically, the frequency of the laser (i.e., the Raman depletion pump) is scanned by varying the drive current linearly. The Raman dip in the power of the Raman laser is observed at a particular point in this scan. A part of the Raman depletion pump is passed through a saturated absorption cell, as also shown in Fig. 1(b). The saturated absorption spectrum is observed during the whole scan. From the known separations

Optics EXPRESS

between the observed resonances, the value of the change in the frequency for a given change in the current is determined. This number is then used to determine the value of Δ_2. The measurements of the values of Δ_1 and Δ_2 are carried out with a precision of ~1 MHz. The measured values are used in the density matrix equations for the simulations. However, this uncertainty in the measurement means that there is an uncertainty of the order of ± 1 MHz in the value of Δ_{AB}. In Fig. 3(a), the location of the dip in the experimental data is lined up with the dip in the theoretical plot as a fitting process.

By matching the amplitude and the linewidth of the Raman depletion in the output power, as well as the laser power away from the dip, we have inferred the expected enhancement as a function of the cavity length change, as shown in Fig. 3(b). The peak value of the enhancement factor is ~1080. To generate Fig. 3(a), the following approach was used. The values of the relevant parameters were estimated by using a combination of measured and known quantities (such as powers in the pump lasers, mode size, output coupler transmissivity and cavity length) and theoretical modeling (which was used to estimate the Rabi frequencies and the optical pumping rate). The parameters were then varied slightly to produce the best fit with the experimental data. Given the complexity of the model, it is difficult to establish quantitatively the degree of uncertainty in the inferred value of the enhancement factor. Only a direct measurement of the enhancement factor would suffice to establish full confidence in the value thereof. As can be seen in Fig. 3(b), the high sensitivity enhancement only happens with very small cavity length perturbations. To measure such a high sensitivity experimentally, over a very narrow range, it is necessary to enhance the stability of the system to ensure that the Raman laser operates at the center of the dip. Currently, work is underway to improve the stability of the system in order to reach this regime.

It is also important to consider the roles of any AC Stark shift of the energy levels, due to the application of the detuned Raman pumps. The Rabi frequencies of the Raman pumps, estimated by weighted averaging over all the allowed magnetic sublevel transitions, are quite small compared to the values of the detunings. Specifically, for the Raman gain pump, the detuning (Δ_1) is 10^9 Hz, while the Rabi frequency (Ω_1) is ~$15.4*10^6$ Hz. Using the fact that the AC Stark shift is approximately ${\Omega_1}^2/4\Delta_1$, we get the shift to be ~59 kHz. For the Raman depletion pump, the detuning (Δ_2) is $1.28*10^9$ Hz, while the Rabi frequency (Ω_2) is ~$14.8*10^6$ Hz. This corresponds to a shift of ~43 kHz.

When the signs of the detunings are taken into account, along with the fact that the shifts are for the upper level in each isotope, the effective values of the hyperfine splittings are found to be 6.834639 GHz (reduced by 43 kHz) for ^{87}Rb and 3.035791 GHz (increased by 59 kHz) for ^{85}Rb. The difference is now 3.798848 GHz, which is 102 kHz smaller than the ideal value of 3.798950 GHz. Thus, the frequency difference between these two pumps has to match this value at the bottom of the dip. As can be seen in Fig. 3(a), the noise in the experimental data tends to mask such a small shift. However, the theoretical model (which includes the effect of the AC Stark shifts naturally, since it employs density matrix equations), to which the experimental data is fitted, shows that the minimum is shifted to the left by ~200 kHz to the left. Thus, while the sign of the shift is consistent with the prediction based on the analysis of the AC Stark shifts summarized above, the actual magnitude of the shift is somewhat different. However, it should be noted that the shift of the minimum away from the ideal location may not be solely due to the AC Stark shift. Since the vertical axis here represents the output laser power, cavity mode pulling may also affect the exact location of the minimum.

In Fig. 4, we have shown comparative theoretical simulation results for two cases: one (red line) in which Δ_1 is positive (with an amplitude of 1 GHz) and Δ_2 is negative (with an amplitude of 1.280 GHz), and the other (blue line) in which the signs of the detunings are reversed. As can be seen, for the latter case, the center of the dip is shifted to the right, by ~500 kHz, while we would expect it to have moved to the right by 102 kHz due to the estimated AC Stark shifts. Thus,

Optics EXPRESS

the signs of the shift in these two cases are consistent with the analysis of the AC Stark shift shown above, but the magnitudes of the shifts are somewhat different from the estimated values. Again, we attribute this quantitative discrepancy to the fact that the shifts may not be solely due to the AC Stark shifts, and possible cavity mode pulling effects need to be analyzed carefully to investigate the source of the discrepancy. More careful analysis of the system, theoretically as well as experimentally, will be carried out in the future to establish clearly the role of the AC Stark shift and the cavity mode pulling effect in the determination of the shift of the minimum away from the ideal location.

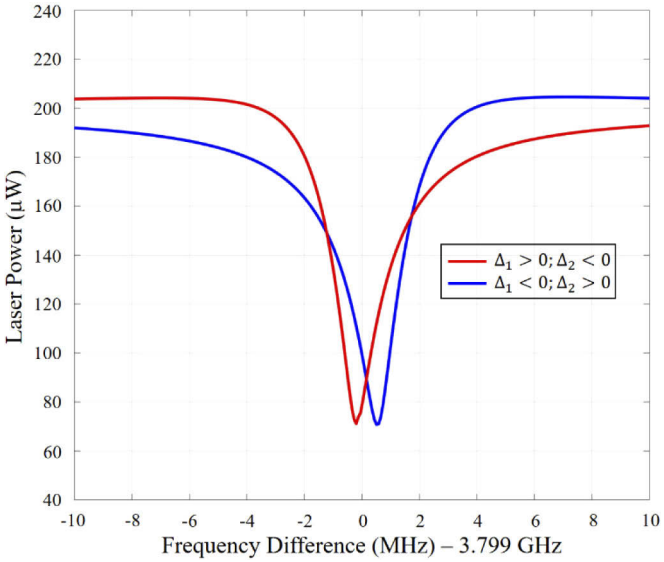

Fig. 4. The asymmetric Raman depletion profiles on both sides of the resonance.

The degree of the spectral asymmetry of the absorption profile depends on the intensity difference between the Raman laser and the Raman depletion pump. For a certain Raman depletion pump power, the stronger the Raman laser beam is, the more asymmetric the absorption profile will be. Moreover, if the signs of Δ_1 and Δ_2 are reversed, the asymmetry will be mirrored across its center, as can be seen in Fig. 4.

5. Summary

To summarize, we have experimentally demonstrated a superluminal Raman laser employing optically pumped Raman gain and self-pumped Raman depletion, with more than a thousand-fold inferred enhancement in sensitivity. If one of the mirrors in the cavity is mounted, for example, on a metallic diaphragm, which transduces acceleration to change in the cavity length, such a laser can be used as a highly sensitive accelerometer. Furthermore, this scheme is suitable for realizing a pair of counter-propagating superluminal lasers in the same cavity without cross-talk. Such a system may be useful for measuring rotation with a sensitivity significantly larger than that of a conventional ring laser gyroscope.

Funding

Air Force Office of Scientific Research (FA9550-18-01-0401, FA9550-18-P-0003); National Aeronautics and Space Administration (80NSSC18P2077); DSCA (PO4440778007).

Optics EXPRESS

References

1. H. N. Yum, M. Salit, J. Yablon, K. Salit, Y. Wang, and M. S. Shahriar, "Superluminal ring laser for hypersensitive sensing," Opt. Express **18**(17), 17658 (2010).
2. M. S. Shahriar, G. S. Pati, R. Tripathi, V. Gopal, M. Messall, and K. Salit, "Ultrahigh enhancement in absolute and relative rotation sensing using fast and slow light," Phys. Rev. A: At., Mol., Opt. Phys. **75**(5), 053807 (2007).
3. G. S. Pati, M. Salit, K. Salit, and M. S. Shahriar, "Demonstration of displacement-measurement-sensitivity proportional to inverse group index of intra-cavity medium in a ring resonator," Opt. Commun. **281**(19), 4931–4935 (2008).
4. D. D. Smith, H. Chang, L. Arissian, and J. C. Diels, "Dispersion-enhanced laser gyroscope," Phys. Rev. A: At., Mol., Opt. Phys. **78**(5), 053824 (2008).
5. J. Scheuer and S. M. Shahriar, "Lasing dynamics of super and sub luminal lasers," Opt. Express **23**(25), 32350 (2015).doi
6. O. Kotlicki, J. Scheuer, and M. S. Shahriar, "Theoretical study on Brillouin fiber laser sensor based on white light cavity," Opt. Express **20**(27), 28234 (2012).
7. H. N. Yum and M. S. Shahriar, "Pump-probe model for the Kramers-Kronig relations in a laser," J. Opt. **12**(10), 104018 (2010).
8. J. Yablon, Z. Zhou, M. Zhou, Y. Wang, S. Tseng, and M. S. Shahriar, "Theoretical modeling and experimental demonstration of Raman probe induced spectral dip for realizing a superluminal laser," Opt. Express **24**(24), 27444 (2016).
9. G. S. Pati, M. Salit, K. Salit, and M. S. Shahriar, "Demonstration of a tunable-bandwidth white-light interferometer using anomalous dispersion in atomic vapor," Phys. Rev. Lett. **99**(13), 133601 (2007).
10. M. S. Shahriar and M. Salit, "Application of fast-light in gravitational wave detection with interferometers and resonators," J. Mod. Opt. **55**(19-20), 3133–3147 (2008).
11. G. S. Pati, M. Salit, K. Salit, and M. S. Shahriar, "Simultaneous slow and fast light effects using probe gain and pump depletion via Raman gain in atomic vapor," Opt. Express **17**(11), 8775 (2009).
12. D. D. Smith, K. Myneni, J. A. Odutola, and J. C. Diels, "Enhanced sensitivity of a passive optical cavity by an intracavity dispersive medium," Phys. Rev. A: At., Mol., Opt. Phys. **80**(1), 011809 (2009).
13. D. D. Smith, H. Chang, K. Myneni, and A. T. Rosenberger, "Fast-light enhancement of an optical cavity by polarization mode coupling," Phys. Rev. A: At., Mol., Opt. Phys. **89**(5), 053804 (2014).
14. K. Myneni, D. D. Smith, H. Chang, and H. A. Luckay, "Temperature sensitivity of the cavity scale factor enhancement for a Gaussian absorption resonance," Phys. Rev. A: At., Mol., Opt. Phys. **92**(5), 053845 (2015).
15. L. J. Wang, A. Kuzmich, and A. Dogariu, "Gain-assisted superluminal light propagation," Nature **406**(6793), 277–279 (2000).
16. P. Kumar and J. H. Shapiro, "Observation of Raman-shifted oscillation near the sodium D lines," Opt. Lett. **10**(5), 226 (1985).
17. M. Poelker and P. Kumar, "Sodium Raman laser: direct measurements of the narrow-band Raman gain," Opt. Lett. **17**(6), 399 (1992).
18. M. S. Shahriar, Y. Wang, S. Krishnamurthy, Y. Tu, G. S. Pati, and S. Tseng, "Evolution of an N -level system via automated vectorization of the Liouville equations and application to optically controlled polarization rotation," J. Mod. Opt. **61**(4), 351–367 (2014).
19. Z. Zhou, J. Yablon, M. Zhou, Y. Wang, A. Heifetz, and M. S. Shahriar, "Modeling and analysis of an ultra-stable subluminal laser," Opt. Commun. **358**, 6–19 (2016).